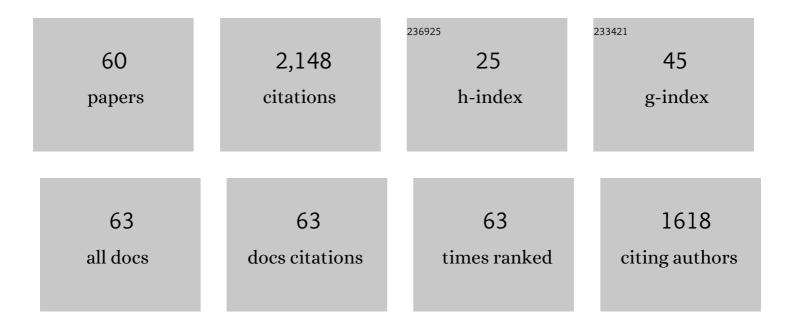
List of Publications by Year in descending order

Source: https://exaly.com/author-pdf/3545431/publications.pdf Version: 2024-02-01



#	Article	IF	CITATIONS
1	Origin and diagenetic priming of a potential slow-slip trigger zone in volcaniclastic deposits flanking a seamount on the subducting plate, Hikurangi margin, New Zealand. New Zealand Journal of Geology, and Geophysics, 2022, 65, 179-200.	1.8	5
2	Effects of coseismic megasplay fault activity on earthquake hazards: Insights from discrete element simulations. Journal of Structural Geology, 2022, 155, 104533.	2.3	0
3	An Improved Earthquake Catalog During the 2018 KıÌ,,lauea Eruption From Combined Onshore and Offshore Seismic Arrays. Earth and Space Science, 2022, 9, .	2.6	2
4	Seafloor overthrusting causes ductile fault deformation and fault sealing along the Northern Hikurangi Margin. Earth and Planetary Science Letters, 2022, 593, 117651.	4.4	6
5	Geometrically controlled slow slip enhanced by seismic waves: A mechanism for delayed triggering. Earth and Planetary Science Letters, 2021, 554, 116695.	4.4	9
6	An OBS Array to Investigate Offshore Seismicity during the 2018ÂKÄ«lauea Eruption. Seismological Research Letters, 2021, 92, 603-612.	1.9	6
7	Relationships Among Forearc Structure, Fault Slip, and Earthquake Magnitude: Numerical Simulations With Applications to the Central Chilean Margin. Geophysical Research Letters, 2021, 48, e2021GL092521.	4.0	1
8	Evidence of Seismic Slip on a Large Splay Fault in the Hikurangi Subduction Zone. Geochemistry, Geophysics, Geosystems, 2021, 22, e2021GC009638.	2.5	6
9	Asymmetric Brittle Deformation at the PÄpaku Fault, Hikurangi Subduction Margin, NZ, IODP Expedition 375. Geochemistry, Geophysics, Geosystems, 2021, 22, e2021GC009662.	2.5	4
10	Can Deep Learning Predict Complete Ruptures in Numerical Megathrust Faults?. Geophysical Research Letters, 2021, 48, e2021GL092607.	4.0	4
11	The Role of Alongâ€Fault Dilatancy in Fault Slip Behavior. Journal of Geophysical Research: Solid Earth, 2021, 126, e2021JB022310.	3.4	8
12	Basal Accretion Along the South Central Chilean Margin and Its Relationship to Great Earthquakes. Journal of Geophysical Research: Solid Earth, 2020, 125, e2020JB019861.	3.4	14
13	Mixed Brittle and Viscous Strain Localization in Pelagic Sediments Seaward of the Hikurangi Margin, New Zealand. Tectonics, 2020, 39, e2019TC005965.	2.8	8
14	Pore Fluid Pressures and Strength Contrasts Maintain Frontal Fault Activity, Northern Hikurangi Margin, New Zealand. Geophysical Research Letters, 2020, 47, e2020GL089209.	4.0	8
15	Slow slip source characterized by lithological and geometric heterogeneity. Science Advances, 2020, 6, eaay3314.	10.3	95
16	Controls on Foreâ€Arc Deformation and Stress Switching After the Great 2011 Tohokuâ€Oki Earthquake From Discrete Numerical Simulations. Journal of Geophysical Research: Solid Earth, 2019, 124, 9265-9279.	3.4	6
17	Microscale Characterization of Fracture Growth and Associated Energy in Granite and Sandstone Analogs: Insights Using the Discrete Element Method. Journal of Geophysical Research: Solid Earth, 2019, 124, 7993-8012.	3.4	11
18	Precursory Stress Changes and Fault Dilation Lead to Fault Rupture: Insights From Discrete Element Simulations. Geophysical Research Letters, 2019, 46, 3180-3188.	4.0	12

#	Article	lF	CITATIONS
19	Microstructural Evolution of Porosity and Stress During the Formation of Brittle Shear Fractures: A Discrete Element Model Study. Journal of Geophysical Research: Solid Earth, 2018, 123, 2228-2245.	3.4	7
20	Recognizing seamount-forearc collisions at accretionary margins: Insights from discrete numerical simulations. Geology, 2017, 45, 635-638.	4.4	40
21	Fault-controlled hydration of the upper mantle during continentalÂrifting. Nature Geoscience, 2016, 9, 384-388.	12.9	75
22	Effects of cohesion on the structural and mechanical evolution of fold and thrust belts and contractional wedges: Discrete element simulations. Journal of Geophysical Research: Solid Earth, 2015, 120, 3870-3896.	3.4	50
23	Galicia Bank ocean–continent transition zone: New seismic reflection constraints. Earth and Planetary Science Letters, 2015, 413, 197-207.	4.4	42
24	Lithospheric flexure and volcano basal boundary conditions: keys to the structural evolution of large volcanic edifices on the terrestrial planets. Geological Society Special Publication, 2015, 401, 219-237.	1.3	18
25	Overview of continuum and particle dynamics methods for mechanical modeling of contractional geologic structures. Journal of Structural Geology, 2014, 59, 19-36.	2.3	37
26	Controls on the size and geometry of landslides: Insights from discrete element numerical simulations. Geomorphology, 2014, 220, 104-113.	2.6	67
27	Eastern Olympus Mons Basal Scarp: Structural and mechanical evidence for largeâ€scale slope instability. Journal of Geophysical Research E: Planets, 2014, 119, 1089-1109.	3.6	10
28	Comparative FEM and DEM modeling of basement-involved thrust structures, with application to Sheep Mountain, Greybull area, Wyoming. Tectonophysics, 2013, 608, 408-417.	2.2	12
29	Insights to slip behavior on rough faults using discrete element modeling. Geophysical Research Letters, 2012, 39, .	4.0	23
30	Rift zone abandonment and reconfiguration in Hawaii: Mauna Loa's Ninole rift zone. Geology, 2010, 38, 471-474.	4.4	5
31	Volcanic spreading and lateral variations in the structure of Olympus Mons, Mars. Geology, 2009, 37, 139-142.	4.4	79
32	Volcanoâ€ŧectonic implications of 3â€D velocity structures derived from joint active and passive source tomography of the island of Hawaii. Journal of Geophysical Research, 2009, 114, .	3.3	31
33	Fault gouge evolution and its dependence on normal stress and rock strength—Results of discrete element simulations: Gouge zone micromechanics. Journal of Geophysical Research, 2008, 113, .	3.3	15
34	Mauna Loa's submarine western flank: Landsliding, deep volcanic spreading, and hydrothermal alteration. Geochemistry, Geophysics, Geosystems, 2007, 8, n/a-n/a.	2.5	17
35	Fault gouge evolution and its dependence on normal stress and rock strength—Results of discrete element simulations: Gouge zone properties. Journal of Geophysical Research, 2007, 112, .	3.3	32
36	The frictional and micromechanical effects of grain comminution in fault gouge from distinct element simulations. Journal of Geophysical Research, 2006, 111, n/a-n/a.	3.3	37

#	Article	IF	CITATIONS
37	Volcanotectonic interactions between Mauna Loa and Kilauea: Insights from 2-D discrete element simulations. Journal of Volcanology and Geothermal Research, 2006, 151, 109-131.	2.1	20
38	Microfossil assemblages on Tuscaloosa Seamount and their constraints on the age of the Nuʻuanu landslide, north of Oahu, HI. Journal of Volcanology and Geothermal Research, 2006, 151, 269-278.	2.1	5
39	Influence of mechanical stratigraphy and initial stress state on the formation of two fault propagation folds. Journal of Structural Geology, 2005, 27, 1954-1972.	2.3	43
40	Discrete element simulations of gravitational volcanic deformation: 1. Deformation structures and geometries. Journal of Geophysical Research, 2005, 110, .	3.3	47
41	Discrete element simulations of gravitational volcanic deformation: 2. Mechanical analysis. Journal of Geophysical Research, 2005, 110, .	3.3	23
42	Internal structure of Puna Ridge: evolution of the submarine East Rift Zone of Kilauea Volcano, HawaiÂÌ€i. Journal of Volcanology and Geothermal Research, 2004, 129, 237-259.	2.1	11
43	Particle Dynamics Simulations of Rate- and State-dependent Frictional Sliding of Granular Fault Gouge. Pure and Applied Geophysics, 2004, 161, 1877.	1.9	46
44	Consolidation state and strength of underthrust sediments and evolution of the décollement at the Nankai accretionary margin: Results of uniaxial reconsolidation experiments. Journal of Geophysical Research, 2004, 109, .	3.3	45
45	Influence of normal stress and grain shape on granular friction: Results of discrete element simulations. Journal of Geophysical Research, 2004, 109, .	3.3	76
46	Olympus Mons aureole deposits: New evidence for a flank failure origin. Journal of Geophysical Research, 2004, 109, .	3.3	93
47	Particle Dynamics Simulations of Rate- and State-dependent Frictional Sliding of Granular Fault Gouge. , 2004, , 1877-1891.		9
48	Slope failure and volcanic spreading along the submarine south flank of Kilauea volcano, Hawaii. Journal of Geophysical Research, 2003, 108, .	3.3	83
49	Volcanic spreading on Mauna Loa volcano, Hawaii: Evidence from accretion, alteration, and exhumation of volcaniclastic sediments. Geology, 2003, 31, 411.	4.4	29
50	Submarine landslides and volcanic features on Kohala and Mauna Kea volcanoes and the Hana Ridge, Hawaii. Geophysical Monograph Series, 2002, , 11-28.	0.1	18
51	Deep-sea volcaniclastic sedimentation around the southern flank of Hawaii. Geophysical Monograph Series, 2002, , 29-50.	0.1	9
52	Structural variability along the submarine south flank of Kilauea volcano, Hawai'i, from a multichannel seismic reflection survey. Geophysical Monograph Series, 2002, , 105-124.	0.1	9
53	Seismic stratigraphy of the Frontal Hawaiian Moat: implications for sedimentary processes at the leading edge of an oceanic hotspot trace. Marine Geology, 2002, 184, 143-162.	2.1	36
54	New insights into deformation and fluid flow processes in the Nankai Trough accretionary prism: Results of Ocean Drilling Program Leg 190. Geochemistry, Geophysics, Geosystems, 2001, 2, n/a-n/a.	2.5	189

#	Article	IF	CITATIONS
55	Overthrusting and sediment accretion along Kilauea's mobile south flank, Hawaii: Evidence for volcanic spreading from marine seismic reflection data. Geology, 2000, 28, 667.	4.4	96
56	Numerical simulations of granular shear zones using the distinct element method: 2. Effects of particle size distribution and interparticle friction on mechanical behavior. Journal of Geophysical Research, 1999, 104, 2721-2732.	3.3	154
57	Numerical simulations of granular shear zones using the distinct element method: 1. Shear zone kinematics and the micromechanics of localization. Journal of Geophysical Research, 1999, 104, 2703-2719.	3.3	225
58	Kinematic constraints on porosity change in the toe of the Cascadia accretionary prism: Evidence for cementation and brittle deformation in the footwall of the frontal thrust. Journal of Geophysical Research, 1997, 102, 15367-15383.	3.3	3
59	Décollement processes at the Nankai accretionary margin, southeast Japan: Propagation, deformation, and dewatering. Journal of Geophysical Research, 1995, 100, 15221-15231.	3.3	51
60	The estimation of diffuse strains in the toe of the western Nankai accretionary prism: A kinematic solution. Journal of Geophysical Research, 1994, 99, 7019.	3.3	26